

Oxygen isotopic and chemical composition of chromites in micrometeorites: Evidence of ordinary chondrite precursors

N. G. Rudraswami^{1*}, Yves Marrocchi², M. Shyam Prasad¹, D. Fernandes¹, Johan Villeneuve², S. Taylor³

¹National Institute Of Oceanography (Council Of Scientific And Industrial Research),
Dona Paula, Goa 403004, India

²CRPG, CNRS, Université De Lorraine, UMR 7358,
Vandoeuvre-Les-Nancy, F-54501, France

³Cold Regions Research And Engineering Laboratory,
72 Lyme Road, Hanover, New Hampshire 03755–1290, USA
Corresponding Author: rudra@nio.org; rudraswami@gmail.com

Abstract

We identified 66 chromite grains from 42 of ~5000 micrometeorites collected from Indian Ocean deep-sea sediments and the South Pole water well. To determine the chromite grains precursors and their contribution to the micrometeorite flux, we combined quantitative electron microprobe analyses and oxygen isotopic analyses by high-resolution secondary ion mass spectrometry. Micrometeorite chromite grains show variable O isotopic compositions with $\delta^{18}\text{O}$ values ranging from -0.8 to 6.0‰ , $\delta^{17}\text{O}$ values from 0.3 to 3.6‰ , and $\Delta^{17}\text{O}$ values from -0.9 to 1.6‰ , most of them being similar to those of chromites from ordinary chondrites. The oxygen isotopic compositions of olivine, considered as a proxy of chromite in chromite-bearing micrometeorites where chromite were too small to be measured in ion microprobe have $\Delta^{17}\text{O}$ values suggesting a principal relationship to ordinary chondritic with some having carbonaceous chondrite precursors. Furthermore, the chemical compositions of chromites in micrometeorites are close to those reported for ordinary chondrite chromites, but some contribution from carbonaceous chondrites cannot be ruled out. Consequently, carbonaceous chondrites cannot be a major contributor of chromite-bearing micrometeorites. Based on their oxygen isotopic and elemental compositions, we thus conclude with no ambiguity that chromite-bearing micrometeorites are largely related to fragments of ordinary chondrites with small fraction from carbonaceous chondrites, unlike other micrometeorites deriving largely from carbonaceous chondrites.

1. Introduction

The Earth's upper atmosphere accretes nearly 30,000 tons of extraterrestrial dust particles (from tens of micrometers to a few millimeters in size) every year: these particles are sourced either from collisions between asteroidal bodies or trails of cometary bodies during perihelion passage (Brownlee 2001). Most (~90%) of these micrometeorites are ablated during atmospheric entry, and only a small percentage reach the Earth's surface intact. They are collected from various environments such as deep-sea sediments (DSS), Antarctic ice, or in the stratosphere during entry and provide information on the varied objects that existed in the early solar system (Love and Brownlee 1993; Taylor et al. 1998; Peucker-Ehrenbrink and Ravizza 2000; Plane 2012; Prasad et al. 2013).

Ordinary chondrites are the most abundant meteorites, accounting for ~80% of all falls (Hutchison, 2004); of those falls, L and H chondrites dominate (~45% each) and ~10% are LL chondrites (Schmitz and Tassinari 2001). This subdivision may preferentially represent the ordinary chondrite component in the inner region of the asteroid belt, where meteorites break down more easily during collisional processes (Meibom and Clark 1999). However, micrometeorites are sourced to a large extent from bodies analogous to carbonaceous chondrites (>70–90%) and probably sample a more diverse population of carbonaceous-type asteroids than represented by meteorites (Love and Brownlee 1993; Beckerling and Bischoff 1995; Brownlee et al. 1997; Yada et al. 2005; Rudraswami et al. 2015a). In addition, a few to ~30% of micrometeorites have asteroidal precursors related to ordinary chondrites, ~1–2% to iron meteorites, and fewer than a percent to HED bodies (Taylor et al. 2007; Suavet et al. 2010; Rudraswami et al. 2015a, b, 2016b).

The chemical compositions of micrometeorites are modified during atmospheric entry, complicating the identification of their precursors based solely on chemical composition. Since oxygen diffuses slower than cations (Ryerson et al. 1989), the oxygen isotopic characteristics of micrometeorites should be better preserved and thus represent a powerful tool for deciphering micrometeorite origins. For instance, oxygen isotopic investigations have indicated the contribution of ordinary chondrites (or precursors analogous to ordinary chondrites) to be only a few percent for micrometeorites sized 100–300 μm (Rudraswami et al. 2015b, 2016a), but ~30% for larger micrometeorites (~600–1000 μm). It should be noted, however, that this size range comprises much less than 1% of the total micrometeorite flux by mass (Suavet et al. 2010).

Chromite is a refractory, high-temperature mineral that is robust to acid treatments and weathering (Schmitz et al. 2001, 2003; Schmitz and Håggström 2006), and spherical to euhedral

chromite grains tens of micrometers in size are largely found in ordinary chondrites. Based on their oxygen isotopic and chemical compositions, it has been proposed that micrometeorite chromites could have largely survived parent-body collisional events, frictional heating during atmospheric entry, and subsequent terrestrial alteration. However, chromite is rarely found in micrometeorites, and earlier studies reported only about a dozen chromite grains among ~500 spherules analyzed, which were conceivably linked to L/H chondrites (Van Ginneken et al. 2012; Prasad et al. 2015). The rarity of chromite grains characterized in micrometeorites limits the information we can obtain on their chemical and isotopic characteristics, and thus the micrometeorite sources in the asteroid belt. Here we determine the chemical and oxygen isotopic compositions of a suite of micrometeorite chromites from DSS and Antarctic ice, and compare their $\Delta^{17}\text{O}$ values with those of ordinary chondrites to assess and distinguish the nature of micrometeorite precursors.

2. Sampling method

Micrometeorites were collected from Indian Ocean DSS and Antarctica. Micrometeorites from Indian Ocean DSS (74–76° E, 10–13° S) were collected using a grab sampler measuring 50 cm long \times 50 cm wide \times 15 cm deep with the capacity to lift 45 kg of sediments from the seafloor depth of ~5000 m (Rudraswami et al. 2011, 2012; Prasad et al. 2013). Retrieved sediments were sieved using a ~200 μm mesh, and further dried and magnetically separated. The estimated terrestrial age of cosmic spherules from DSS at 0–15 cm depth based on the peak tektite abundance from three sediment cores is ~0–50,000 a (Prasad et al. 2013). Antarctic micrometeorites were collected from the South Pole water well that supplies water to the Amundsen-Scott South Pole Station. The 24 m diameter well is situated at ~100 m below the surface, contains ~5000 m^3 of melt water, and extends to 16 m depth below the well opening (Taylor et al. 1998, 2000). Particles from the well bottom were suctioned by a sample collector and sieved to various size fractions $>50 \mu\text{m}$. A binocular microscope was used to pick and mount samples in epoxy for analyses. Antarctic and DSS micrometeorites were mounted on 2 and 16 epoxy mounts, respectively, and polished to expose their surface diametrically. The sections were cleaned using alcohol and distilled water in an ultrasonic bath, then dried. Each section was carbon coated for observation under a scanning electron microscope (SEM) to identify chromites before chemical and isotopic characterization by electron and ion microprobe, respectively.

3. Analytical techniques

3.1. Electron microscopy and microprobe analyses

SEM and microprobe analyses were performed at the National Institute of Oceanography (Goa, India). A JEOL JSM-IT300LV SEM equipped with an energy dispersive spectrometer (AZtecEnergy EDS Microanalysis, Oxford instruments) was used to identify chromites in the micrometeorites and obtain back-scattered electron images. Chromite-bearing micrometeorites were further analyzed using a Cameca SX5 Electron Micro Probe Analyzer equipped with four spectrometers. Microprobe analyses were performed with ~15 kV accelerating voltage, ~12 nA beam current, and ~1–2 μm beam diameter. The PAP model was used for matrix corrections (Pouchou and Pichoir 1991). Multiple analyses were performed on each spherule containing different mineral phases to obtain bulk chemical compositions by calculating the exposed area of different mineral phases in ImageJ or LISPIX. We note that the reported bulk compositions do not account for density differences among phases. For scoriaceous, barred, cryptocrystalline, or glassy micrometeorites, several analyses were performed using a ~5 μm beam diameter and averaged to obtain the bulk chemical composition; the beam size was restricted to 5 μm to avoid void spaces, vesicles, and pits. To improve the accuracy and statistical error on minor element measurements (Ca, V, Mn, Ti, Zn), analyses were performed with long counting times of 60 s on peak and 20 s on background. Replicate measurements of multiple standards were within 1% error for major elements and within a few percent for minor elements. Multiple analyses were performed at different spots in each chromite grain to constrain their chemical heterogeneity.

3.2. Oxygen isotopic analyses

Oxygen isotopic analyses of micrometeorite olivine (here representing the micrometeorite composition) and chromite phases were performed using a Cameca 1270 E7 at CRPG-CNRS (Nancy, France) using a Cs^+ beam with ~1 nA primary current and ~5 μm beam spot on the sample surface. We used a mass resolving power of ~2500 for ^{16}O and ^{18}O and ~7000 for ^{17}O to avoid $^{16}\text{OH}^-$ interference in the ^{17}O peak. Secondary ^{16}O and ^{18}O ions were measured using a faraday cup while ^{17}O was measured using the electron multiplier in multi-collection mode. We corrected for instrumental mass fractionation in olivine grains using San Carlos olivine. Stillwater chromite (Schmitz et al., 2016) and UWCr-3 chromite standards were used to check the stability and reproducibility of the isotopic data (Heck et al. 2010), and the Stillwater chromite was used as a running standard for unknown chromite grains. Typical count rates obtained on the Stillwater chromite standard were $\sim 5 \times 10^8$ cps for ^{16}O , $\sim 2 \times 10^5$ cps for ^{17}O , and $\sim 1 \times 10^6$ cps for ^{18}O . Typical

errors (2σ), accounting for measurement errors and the external reproducibility of the standard, are estimated to be $\sim 0.7\text{‰}$ for $\delta^{18}\text{O}$, $\sim 0.6\text{‰}$ for $\delta^{17}\text{O}$, and $\sim 0.8\text{‰}$ for $\Delta^{17}\text{O}$ ($= \delta^{17}\text{O} - 0.52 \times \delta^{18}\text{O}$, representing deviation from the terrestrial fractional line). All analytical spots were checked under SEM, and any that fell on cracks or grain boundaries were excluded.

4. Results

We examined ~ 3500 DSS micrometeorites and ~ 1500 Antarctic micrometeorites to identify chromite-bearing micrometeorites for further understanding the chemical and isotopic characteristics of these particles. We found 46 chromites in 30 DSS micrometeorites and 20 chromites in 12 Antarctic micrometeorites; the chemical compositions and sizes of these chromites are reported in Table 1. Chromite grains varied from round to euhedral (Figs. 1 and 2). Most of the chromite-bearing micrometeorites displayed barred, cryptocrystalline, glass, or porphyritic type textures (Figs. 1 and 2). Only two chromite grains were observed in partially melted scoriaceous particles, and their small sizes made their isotopic characterization challenging. Some chromites may have been altered, as their Si, Mg, Al, and Fe contents were slightly modified due to heating during atmospheric entry, but nonetheless seem to largely retain their elemental compositions. Fig. 3 shows the sizes (maximum length) of chromite grains relative to their major axes of their host micrometeorites as well as the distribution of chromite grain sizes. Most chromites are between ~ 5 and $100\ \mu\text{m}$ in their maximum dimension, though some altered chromites are smaller, between a few and $<10\ \mu\text{m}$ (Fig. 2).

We selected 18 micrometeorites for oxygen isotopic analyses of chromite and olivine grains. In nine micrometeorites larger than $20\ \mu\text{m}$, we analyzed the oxygen isotopic compositions of olivines and 17 chromites (Table 2); in the other nine, chromites were too small to analyze, so we measured the oxygen isotopic compositions of olivines only. The $\delta^{18}\text{O}$ and $\delta^{17}\text{O}$ values of chromite grains range from -0.8 to 6.0‰ and from 0.3 to 3.6‰ , respectively, corresponding to $\Delta^{17}\text{O}$ values of -0.9 to 1.6‰ (Figs. 4–6). Micrometeorite olivines have the same limited range of $\Delta^{17}\text{O}$ values, except for a few that fall near carbonaceous chondrite. The $\Delta^{17}\text{O}$ values reported for micrometeorite olivines and chromites in Figs. 5 and 6 are averaged per micrometeorite, assuming that individual micrometeorites document a single precursor.

5. Discussion

Chromites in micrometeorites provide powerful constraints on heating during atmospheric entry and micrometeorite precursors. The mere presence of chromite is insufficient to distinguish

between the different types of chondrites or metamorphic grades (Bunch et al. 1967; Johnson and Prinz 1991), though chromites can be used to validate analogous micrometeorite precursors. For example, Prasad et al. (2015) used chemical composition as analytical tool for the chromites in micrometeorites to show that four of seven micrometeorites were related to L3–6 chondrites, and the remaining three to a combination of L/H-type chondrites. However, such a small number of chromite grains is not statistically robust enough to conclusively identify their sources. Here, we broaden the statistics from the different sampling sites (DSS and Antarctic ice), and include micrometeorites of a larger size range (50–500 μm) that arrived on Earth during the past $\sim 50,000$ years (Taylor et al. 1998; Prasad et al. 2015). Our detailed investigation of the oxygen isotopic compositions and physical and chemical properties of chromites will improve our understanding of the parent bodies of chromite-bearing micrometeorites and their contributions to the micrometeorite flux.

5.1 Origin of chromite-bearing micrometeorites

Chromite size has not shown any particular trend with respect to micrometeorite size, however, it seems to be negatively correlated to chromite abundance; i.e., the chromite grains observed herein range in size from 4 to 153 μm , but are largely dominated by $\sim 5\text{--}50$ μm grains from micrometeorites $\sim 50\text{--}500$ μm in size (Fig. 3). Chromites are present in carbonaceous chondrites, but are typically smaller than those in ordinary chondrites (Johnson and Prinz, 1991). In L-type chondrites, chromite sizes vary according to the different metamorphic grades (L3, $\sim 10\text{--}50$ μm ; L4, $\sim 18\text{--}150$ μm ; L5, $\sim 25\text{--}160$ μm ; and L6, $\sim 30\text{--}600$ μm ; Bridges et al. 2007), and the sizes of the largest chromite grains observed increase with increasing petrographic grade. Based on these size distributions, our results suggest that the chromite-bearing micrometeorites reported herein could derive from ordinary chondrites. However, chromite size alone is not diagnostic of chondrite type or metamorphic grade, and these results must be coupled with the chemical and O isotopic compositions of chromites to convincingly relate them to specific chondrite types.

Chromite is the most abundant spinel group mineral in ordinary chondrites (up to 0.6 wt%; Keil 1962) and the least abundant in carbonaceous chondrites (<0.01 wt%; Riebe 2009). In addition, chromites in ordinary chondrites have more varied chemical compositions than those in carbonaceous chondrites, likely due to the increased thermal metamorphism of ordinary chondrite parent bodies compared to carbonaceous ones. The concentrations of minor oxide such as TiO_2 , MnO , Cr_2O_3 , V_2O_5 , or ZnO are therefore powerful tools for ascertaining the chondritic provenance of chromites, although chemical overlaps are observed. Chromites in H chondrites have very restricted TiO_2 contents ranging from ~ 1.5 to 3.0 wt%, LL chondrites have higher TiO_2 contents of

~2.5–4.5 wt%, and L chondrites show the widest range, from 0.5 to 3.5 wt% TiO₂ (Fig. 7). In general, the average TiO₂ content of equilibrated grains increases from H to L to LL chondrites. The least metamorphosed L3 chondrites have chromites with <2 wt% TiO₂, similar to the much smaller chromites in carbonaceous chondrites (< 2 wt% TiO₂; Fuchs et al. 1973; Johnson and Prinz, 1991). Our data largely matches the range of chromite TiO₂ contents observed in ordinary chondrites, and to some extent that in carbonaceous chondrites.

Furthermore, chromites in ordinary chondrites are enriched in MnO (0.5–0.95 wt%) relative to those in carbonaceous chondrites (0.0–0.2 wt%; Bunch et al. 1967; Wlotzka 2005). Among ordinary chondrites, chromites in H chondrites are Mn-enriched (~0.9 wt%) relative to those in L (~0.7 wt%) and LL chondrites (~0.5 wt%; Bunch et al. 1967; Wlotzka 2005). Our results show that micrometeorite chromites are relatively rich in MnO (0.03–0.63 wt%, averaging 0.32 ± 0.16 wt% MnO; Table 1, Fig. 8), suggesting that micrometeorites could have derived from ordinary with some from carbonaceous chondrites. Most of the data in Fig. 8 show scattered data that make difficult to assert the precursor with great confidence. Apart from this, the diffusion of the minor element that has taken place during entry makes the matter worse to identify the precursor. This is supported by (i) V₂O₃ vs. Cr₂O₃, MnO, and TiO₂ plots indicate a larger fraction of micrometeorite chromite grains plot in the area of ordinary chondrite chromites with relatively small fraction in the carbonaceous chondrite range (Fig. 8), and (ii) micrometeorite chromite ZnO concentrations up to 0.3 wt%, beyond the range of the systematically Zn-poor carbonaceous chondrite chromites (<0.1 wt% ZnO; Fuchs et al. 1973; Brearley and Jones 1998).

The oxygen isotopic compositions of micrometeorite chromites allow determination of the contribution of chromite-bearing extraterrestrial material to the Earth's surface. The ordinary and enstatite chondrite have $\Delta^{17}\text{O}$ lying between 0.1 and 1.5‰, while the carbonaceous chondrite have wider range with $\Delta^{17}\text{O}$ <0‰, for e.g. CV chondrite having –5 to –1‰, CO and CK having –5 to –4‰, CR having –2 to –1‰, CM having –4 to –1‰, respectively (Clayton et al., 1991, 1999) Our results show that micrometeorite chromites have ¹⁶O-poor isotopic compositions similar to those measured in ordinary chondrites (Table 2; Clayton et al. 1991; Greenwood et al. 2007). One of our micrometeorites (SP005-P219) has a chromite grain with a slightly ¹⁶O-rich composition ($\Delta^{17}\text{O}$ values ranging from –0.3 to –0.9‰), and thus probably derives from a carbonaceous chondrite (Table 2). Excluding this micrometeorite, all other chromite grains observed seems to originate predominately with oxygen isotopic compositions very similar to those of chromites in ordinary chondrites. It may be difficult based on the oxygen isotope studies of chromites to narrow on specific population of ordinary

chondrite. Nevertheless, our results indicate that chromites are dominantly related to ordinary chondrites, and that the contribution from carbonaceous chondrites is small (Figs. 4–6).

The O isotopic compositions of olivines in micrometeorites with chromite grains too small for ion microprobe analyses indicate that most of the micrometeorites have ordinary chondrite compositions, while about six have shown $\Delta^{17}\text{O} < 0$ (Fig. 6). The negative $\Delta^{17}\text{O}$ values for these chromite-bearing micrometeorites point toward mainstream contribution from ordinary chondrite with some from carbonaceous chondrites. Many of the micrometeorites have undergone alteration during atmospheric entry, as attested by their high $\delta^{17,18}\text{O}$ values that result from exchange with the stratospheric oxygen isotope composition of $\delta^{18}\text{O} = 23.5\text{‰}$, and $\delta^{17}\text{O} = 11.8\text{‰}$ (Thiemens et al., 1995; Engrand et al. 2005; Yada et al. 2005; Suavet et al. 2010; Cordier et al. 2011; Rudraswami et al. 2015a, 2016a). However, their $\Delta^{17}\text{O}$ values are similar to those reported for chromite grains in ordinary chondrites, in contrast to many micrometeorites analyzed previously that were dominated by carbonaceous chondrite compositions (Clayton et al. 1991; Engrand et al. 1999; Greenwood et al. 2007; Rudraswami et al. 2015a, 2016a). Excluding the few dataset that has shown us $\Delta^{17}\text{O}$ in carbonaceous chondrite range, these results support the conclusion that chromite grains have O-isotopic compositions similar to ordinary chondrites. Though oxygen isotopic exchange between chromite-bearing micrometeorites and the atmosphere during entry resulted in $\delta^{17,18}\text{O}$ values shifted towards atmospheric values in many olivine grains, the O isotopic compositions of chromite grains indicate that they are resistive and retain their precursor, i.e., ordinary chondritic, composition (Figs. 4–6).

5.2 Implications for asteroid belt dynamics

The chemical and mineralogical compositions of interplanetary dust particles and micrometeorites show strong similarities to those of carbonaceous chondrites, unlike meteorites that are dominated by ordinary chondrites (Brownlee et al. 1997; Rietmeijer 1998; Schmitz and Tassinari 2001). This discrepancy may be due to the dominance of ordinary chondrite bodies in the inner asteroid belt, where slight planetary perturbations can send larger asteroidal bodies into Earth resonant orbits, eventually reaching Earth as ordinary chondrite meteorites (Meibom and Clark 1999). This is not the case with micrometeorites; small dust particles generated by collisions can arrive in Earth resonant orbits from any region of the asteroid belt. It thus appears that the diversity of planetary bodies present in the asteroid belt is better represented in the micrometeorite flux, which exceeds that of meteorites and is therefore more statistically significant.

Although our study clearly indicates a genetic link between ordinary chondrites and many chromite-bearing micrometeorites, the latter constitute only ~1% of micrometeorites collected from DSS and Antarctic ice. Antarctic micrometeorites have terrestrial ages of ~1000 a (Taylor et al. 1998), whereas micrometeorites in DSS are as old as ~50,000 a (Prasad et al. 2013). In these two time spans (Taylor et al., 1998; Prasad et al., 2013), the flux of chromite-bearing micrometeorites has remained almost constant and no major collision event has been reported in the recent past. The abundance of micrometeorites related to ordinary chondrites is probably underestimated due to the non-systematic presence of chromite grains in micrometeorites derived from ordinary chondrites. Nevertheless, it seems that ordinary chondrites are rare in the asteroid belt, which is rather dominated by carbonaceous bodies as reflected in the chemical and isotopic compositions of micrometeorites (Brownlee et al. 1997; Meibon and Clark 1999; Taylor et al. 2007; Genge et al. 2008; Suavet et al. 2010; Rudraswami et al. 2012, 2014, 2015b, 2016b). This could be due to either (i) a population deprived of S-type asteroids in the asteroid belt or (ii) an under-representation of dust related to ordinary chondrites in Earth resonant orbits.

The predominance of micrometeorites derived from carbonaceous chondrites could also result from the large differences in the physical properties of carbonaceous and ordinary chondrites, such as tensile strength, density, and porosity. Tensile strength is a critical parameter controlling the dust sizes generated during collisions; the greater the tensile strength, the larger the collisional debris (Flynn et al. 1999; Consolmagno et al. 2008). Furthermore, the lower porosity of ordinary compared to carbonaceous chondrites would generate larger particles during asteroid breakup. Disruptive impact experiments performed on different chondrite types revealed that carbonaceous chondrites produce more fragments in the micrometeorite mass range than ordinary chondrites (Flynn et al. 2009). These results suggest that the physical properties of carbonaceous chondrites (i.e., high porosity, low density and tensile strength) induce fragmentation into dust-sized particles during asteroidal collisions (Consolmagno et al. 2008). This is consistent with the large contribution of micrometeorites from carbonaceous chondrites, whereas there is a disparity in the ordinary chondrite contribution that varies from a few percent for smaller sizes (<300 μm) to ~30% for larger sizes (>600 μm) (e.g., Suavet et al. 2010; Rudraswami et al. 2015b, 2016b). The porosity (10–17%) and density (3.0–3.2 g/cm^3) of the higher petrographic grade L chondrites (L5 and L6) are similar to those of carbonaceous chondrites such as CO3 and CV3, and the increased porosity (up to 23%) and decreased density (up to 2.6 g/cm^3) at lower petrographic grades are being listed as similar to those reported for many primitive carbonaceous chondrites (Flynn et al. 1999). H and LL chondrites, however, have porosities much lower than those of L5–6 or H5–6 chondrites, even at lower

petrographic (e.g., LL3) grades (Flynn et al. 1999). Overall, the high porosity and low density of L-type chondrites compared to other ordinary chondrites favor fragmentation into smaller dust particles during collisions, although our present dataset does not allow us to conclusively relate micrometeorites to a petrographic grade or type of ordinary chondrite.

6. Conclusions

In-situ oxygen isotopic analyses of chromite-bearing micrometeorites revealed that chromites in micrometeorites are indistinguishable from those in ordinary chondrites. The $\Delta^{17}\text{O}$ values of most chromite-bearing micrometeorites here and in the literature are similar to those of ordinary chondrites, indicating that chromite-bearing micrometeorites are largely derived from ordinary chondrites (~70%) with small contribution (~30%) from carbonaceous chondrites. Chromite chemical compositions support an ordinary chondrite provenance despite the chemical compositions of some chromites being altered during atmospheric entry, as reflected by compositions enriched in Si, Mg, Al, and Fe. The two time spans analyzed herein (the last ~1000 and ~50,000 years in DSS and Antarctic ice, respectively) suggest that the contribution of chromite-bearing micrometeorites related to ordinary chondrites in the size range ~50–500 μm has remained consistent at ~1% of the total micrometeorite flux during the last 50,000 years. The low overall abundance of micrometeorites related to ordinary chondrites likely indicates a small contribution of ordinary chondrites to dust particles produced in the asteroid belt.

Acknowledgements

This work was funded by GEOSINKS, MOES-PMN, and the PLANEX project. The National Science Foundation funded the collection of micrometeorites from the South Pole water well. We acknowledge the support of Vijay Khedekar, Areef Sardar, and Lionel G. Vacher for electron microscopy. We thank John Valley, Noriko Kita, and Kazu Nagashima for providing the chromite standards used in this study. This is NIO's contribution No. xxxx.

References

- Beckerling W. and Bischoff A. 1995. Occurrence and composition of relict minerals in micrometeorites from Greenland and Antarctica—implications for their origins. *Planetary and Space Science* 43:435-449.
- Brearley A. J. and Jones R. H. 1998. Chondritic meteorites. In *Planetary materials*, edited by Papike J. J. Reviews in Mineralogy, vol. 36. Washington, D.C.: Mineralogical Society of America. pp. 1- 398.

- Bridges J. C., Schmitz B., Hutchison R., Greenwood R. C., Tassinari M., and Franchi I. A. 2007. Petrographic classification of mid-Ordovician fossil meteorites from Sweden. *Meteoritics & Planetary Science* 42:1781–1789.
- Brownlee D. E. 2001. The origin and properties of dust impacting the Earth. In *Accretion of extraterrestrial matter throughout Earth's history*, edited by Peucker-Ehrenbrink B. and Schmitz B. New York: Kluwer/Plenum. pp. 1–12.
- Brownlee D. E., Bates B., and Schramm L. 1997. The elemental composition of stony cosmic spherules. *Meteoritics & Planetary Science* 32:157–175.
- Bunch T. E., Keil K., and Snetsinger K. G. 1967. Chromite composition in relation to chemistry and texture of ordinary chondrites. *Geochimica et Cosmochimica. Acta* 31:569–1582.
- Clayton R. N., Mayeda T. K., Goswami J. N. and Olsen E. J. 1991. Oxygen isotope studies of ordinary chondrites. *Geochimica et Cosmochimica. Acta* 55:2317–2337.
- Consolmagno G. J., Britt D.T., and Macke R. J. 2008. The significance of meteorite density and porosity. *Chemie der Erde* 68:1–29.
- Cordier C., Folco L., Suavet C., Sonzogni C., and Rochette P. 2011. Major, trace element and oxygen isotope study of glass cosmic spherules of chondritic composition: The record of their source material and atmospheric entry heating. *Geochimica et Cosmochimica. Acta* 75:5203–5218.
- Engrand C., McKeegan K. D., and Leshin L. A. 1999. Oxygen isotopic compositions of individual minerals in Antarctic micrometeorites: Further links to carbonaceous chondrites. *Geochimica et Cosmochimica. Acta* 63:2623–2636.
- Engrand C., McKeegan K. D., Leshin L.A., Herzog G.F., Schnabel C., Nyquist L.E., and Brownlee D. E. 2005. Isotopic compositions of oxygen, iron, chromium, and nickel in cosmic spherules: toward a better comprehension of atmospheric entry heating effects. *Geochimica et Cosmochimica. Acta* 69:5365–5385.
- Flynn G. J., Durda D. D., Sandel L. E., Kreft J. W., and Strait M. M. 2009. Dust production from the hypervelocity impact disruption of the Murchison hydrous CM2 meteorite: implications for the disruption of hydrous asteroids and the production of interplanetary dust. *Planetary and Space Science* 57:119–126.
- Flynn G.J., Moore L.B., and Klöck W. 1999. Density and Porosity of Stone Meteorites: Implications for the Density, Porosity, Cratering, and Collisional Disruption of Asteroids. *Icarus* 142:97–105.
- Fuchs L.H., Olsen E., and Jensen K. J. 1973. Mineralogy, mineral chemistry, and composition of the Murchison (C2) meteorite. *Smithsonian Contribution to Earth Sciences* 10:1–39.
- Genge M. J., Engrand C., Gounelle M., and Taylor S. 2008. The classification of micrometeorites. *Meteoritics & Planetary Science* 43: 497–515.

- Greenwood R. C., Schmitz B., Bridges J. B., Hutchison R. W., and Franchi I. A. 2007. Disruption of the L-chondrite parent body: new oxygen isotope evidence from Ordovician relict chromite grains. *Earth and Planetary Science Letters* 262:204–213.
- Heck P. R., Ushikubo T., Schmitz B., Kita N. T., Spicuzza M. J., and Valley J. W. 2010. A single asteroidal source for extraterrestrial Ordovician chromite grains from Sweden and China: high-precision oxygen three-isotope SIMS analysis. *Geochimica et Cosmochimica. Acta* 74:497–509.
- Hutchison R. 2004. *Meteorites. A petrologic, chemical and isotopic synthesis*. Cambridge, UK: Cambridge University Press. 506 p.
- Johnson C. A. and Prinz M. 1991. Chromite and olivine in type II chondrules in carbonaceous and ordinary chondrites: implications for thermal histories and group differences. *Geochimica et Cosmochimica. Acta* 55:893–904.
- Keil K. 1962. On the phase composition of meteorites. *Journal of Geophysical Research* 67: 4055–61.
- Love S. G. and Brownlee D. E. 1993. A direct measurement of the terrestrial mass accretion rate of cosmic dust. *Science* 262:550–553.
- Meibom A. and Clark B. E. 1999. Evidence for the insignificance of ordinary chondritic material in the asteroid belt. *Meteoritics & Planetary Science* 34:7–24.
- Peucker-Ehrenbrink B. and Ravizza G. 2000. The effects of sampling artifacts on cosmic dust flux estimates: a reevaluation of nonvolatile tracers (Os, Ir). *Geochimica et Cosmochimica. Acta* 64:1965–1970.
- Plane J.M.C. 2012. Cosmic dust in the earth’s atmosphere. *Chemical Society Reviews* 41: 6507–6518.
- Pouchou J. L. and Pichoir F. 1991. Quantitative analysis of homogeneous or stratified microvolumes applying the model “PAP”. In *Electron Probe Quantification*, edited by Heinrich K. F. J. and Newbury D. E. New York: Plenum Press. pp. 31–75.
- Prasad M. S., Rudraswami N. G., Araujo A., Babu E.V.S.S.K., and Vijaya Kumar T. 2015. Ordinary chondritic micrometeorites from the Indian Ocean. *Meteoritics & Planetary Science* 50:1013–1031.
- Prasad M. S., Rudraswami, N. G., and Panda D. K. 2013. Micrometeorite flux on earth during the last ~50,000 years. *Journal of Geophysical Research* 118: 2381–2399.
- Riebe M. 2009. Spinel Group Minerals in Carbonaceous and Ordinary Chondrites. B.A. thesis, Lund University, Lund, Sweden.
- Rietmeijer F.J.M. 1998. Interplanetary Dust Particles. In *Planetary materials* edited by Papike J. J. Reviews in Mineralogy, vol. 36. Washington, D.C.: Mineralogical Society of America. p. 95.

- Rudraswami N. G., Parashar K., and Shyam Prasad M. 2011. Micrometer and nanometer size platinum group nuggets in micrometeorites from the deep sea sediments of Indian Ocean. *Meteoritics & Planetary Science* 46:470–491.
- Rudraswami N. G., Shyam Prasad M., Jones R. H., and Nagashima K. 2016a. In situ oxygen isotope compositions in olivines of different types of cosmic spherules: An assessment of relationships to chondritic particles. *Geochimica et Cosmochimica. Acta* 194:1–14.
- Rudraswami N. G., Shyam Prasad M., Dey S., Plane J. M. C., Feng W., Carrillo-Sánchez J. D., and Fernandes D. 2016b. Ablation and Chemical Alteration of Cosmic Dust Particles during Entry into the Earth's Atmosphere. *The Astrophysical Journal Supplement Series* 227:15.
- Rudraswami N. G., Prasad M. S., Nagashima K., and Jones R. H. 2015a. Oxygen isotopic composition of relict olivine grains in cosmic spherules: Links to chondrules from carbonaceous chondrites. *Geochimica et Cosmochimica. Acta* 164:57-70.
- Rudraswami N. G., Shyam Prasad M., Dey S., Plane J. M. C., Feng W., and Taylor S. 2015b. Evaluating changes in the elemental composition of micrometeorites during entry into the Earth's atmosphere. *The Astrophysical Journal* 814:78.
- Rudraswami N.G., Shyam Prasad M., Babu E.V.S.S.K., and Vijaya Kumar T. 2014. Chemistry and petrology of Fe-Ni beads from different types of cosmic spherules: Implication for precursors. *Geochimica et Cosmochimica. Acta* 145:139-158.
- Rudraswami N.G., Shyam Prasad M., Babu E.V.S.S.K., Vijaya Kumar T., Feng W., and Plane J.M.C. 2012. Fractionation and fragmentation of glass cosmic spherules during atmospheric entry. *Geochimica et Cosmochimica. Acta* 99:110–127.
- Ryerson F.J., Durham W.B., Cherniak D.J., and Lanford W.A. 1989. Oxygen diffusion in olivine: effect of oxygen fugacity and implications for creep. *Journal of Geophysical Research* 94:4105–4118.
- Schmitz B. and Häggström T. 2006. Extraterrestrial chromite in Middle Ordovician marine limestone at Kinnekulle, southern Sweden—Traces of a major asteroid breakup event. *Meteoritics & Planetary Science* 41:455–466.
- Schmitz B. and Tassinari M. 2001. Fossil meteorites. In *Accretion of extraterrestrial matter throughout Earth's history*, edited by Peucker-Ehrenbrink B. Schmitz B. New York: Kluwer Academics pp. 319–331.
- Schmitz B., Häggström T., and Tassinari M. 2003. Sediment-dispersed extraterrestrial chromite traces a major asteroid disruption event. *Science* 300:961–964.
- Schmitz B., Tassinari M., and Peucker-Ehrenbrink B. 2001. A rain of ordinary chondritic meteorites in the early Ordovician. *Earth and Planetary Science Letters* 194:1–15.
- Schmitz B., Yin Q.-Z., Sanborn M.E., Tassinari M., Caplan C. E., and Huss G.R., 2016. A new type of solar-system material recovered from Ordovician marine limestone. *Nature Communications* 7, 11851.

- Snetsinger K. G., Keil K., and Bunch T.E. 1967. Chromite from 'equilibrated' chondrites, *American Mineralogist* 52:1322–1331.
- Suavet C., Alexandre A., Franchi I. A., Gattacceca J., Sonzogni C., Greenwood R. C., Folco L., and Rochette P. 2010. Identification of the parent bodies of micrometeorites with high-precision oxygen isotope ratios. *Earth and Planetary Science Letters* 293:313–320.
- Taylor S., Herzog G. F., and Delaney J. S. 2007. Crumbs from the crust of Vesta: achondritic cosmic spherules from the South Pole water well. *Meteoritics & Planetary Science* 42:155–304.
- Taylor S., Lever J. H., and Harvey R. P. 1998. Accretion rate of cosmic spherules measured at the South Pole. *Nature* 392, 899–903.
- Taylor S., Lever J. H., and Harvey R. P. 2000. Numbers, types and compositions of an unbiased collection of cosmic spherules. *Meteoritics & Planetary Science* 35:651–666.
- Van Ginneken M., Folco L., Cordier C., and Rochette P. 2012. Chondritic micrometeorites from the Transantarctic Mountains. *Meteoritics & Planetary Science* 47:228–247.
- Wlotzka F. 2005. Cr spinel and chromite as petrogenetic indicators in ordinary chondrites: equilibration temperatures of petrologic types 3.7 to 6. *Meteoritics & Planetary Science* 40:1673–1702.
- Yada T., Nakamura T., Noguchi T., Matsumoto N., Kusakabe M., Hiyagon H., Ushikubo T., Sugiura N., Kojima H., and Takaoka N. 2005. Oxygen isotopic and chemical compositions of cosmic spherules collected from the Antarctic ice sheet: implications for their precursor materials. *Geochimica et Cosmochimica. Acta* 69:5789–5804.

Figure Captions

Figure 1.

Representative back-scattered electron images of chromite-bearing micrometeorites collected from Indian Ocean DSS and the South Pole water well (SPWW). Chromites are circled in each image. The chemical compositions of chromites unaffected by atmospheric entry are given in Table 1.

Figure 2.

Enlarged back-scattered electron images of chromites in micrometeorites.

Figure 3.

(a) Chromite sizes as a function of their host relict micrometeorites. (b) The size distribution of chromites from micrometeorites analyzed in this study.

Figure 4.

The oxygen isotopic compositions of olivines (representing micrometeorites) and chromites in chromite-bearing micrometeorites. Data points represent individual analyses. Most of them are depleted in ^{16}O and have $\Delta^{17}\text{O}$ values similar to those of ordinary chondrites. The TF and Carbonaceous Chondrite Anhydrous Mineral (CCAM) lines are shown for reference. The error bars of many of the data points are masked by the size of the data points themselves.

Figure 5.

$\Delta^{17}\text{O}$ versus $\delta^{18}\text{O}$ values of chromites in chromite-bearing micrometeorites. Chromite compositions are averaged per micrometeorite depending on the number of oxygen isotope analyses which varies from two to three chromite per micrometeorite, however, there are few that only represent single analyses. Most of the data fall in the ordinary chondrite range, as delimited by the range of $\Delta^{17}\text{O}$ values of LL, L, and H chondrites (green, blue, and red lines, respectively).

Figure 6

The distribution of average $\Delta^{17}\text{O}$ values of 18 chromite-bearing micrometeorites (gray). Chromites were large enough to analyze in nine of those micrometeorites (black), and the values shown are averaged per micrometeorite.

Figure 7.

The distribution of TiO_2 contents in chromites from (a) micrometeorites studied herein and (b) different chondrite types (carbonaceous, L, LL, H). Data for chromites from ordinary chondrites are from Bunch et al. (1967), Snetsinger et al. (1967), Johnson and Prinz (1991), and Wlotzka (2005). Data for chromites from carbonaceous chondrites are from Fuchs et al. (1973) and Johnson and Prinz (1991).

Figure 8.

Elemental distributions of chromites from micrometeorites studied herein (red), carbonaceous chondrites (yellow) and ordinary (L, LL, and H) chondrites (gray diamonds, inverted triangles, and circles, respectively). Data for chromites from ordinary chondrites are from Bunch et al. (1967), Snetsinger et al. (1967), Johnson and Prinz (1991), and Wlotzka (2005). Data for chromites from carbonaceous chondrites are from Fuchs et al. (1973) and Johnson and Prinz (1991). The rectangle and oval outline represent the spread in data of chromite from ordinary and carbonaceous chondrites, respectively. In figs. a, c, d, f, the H chondrite has shown narrow spread and are marked with smaller rectangle.

Fig. 1

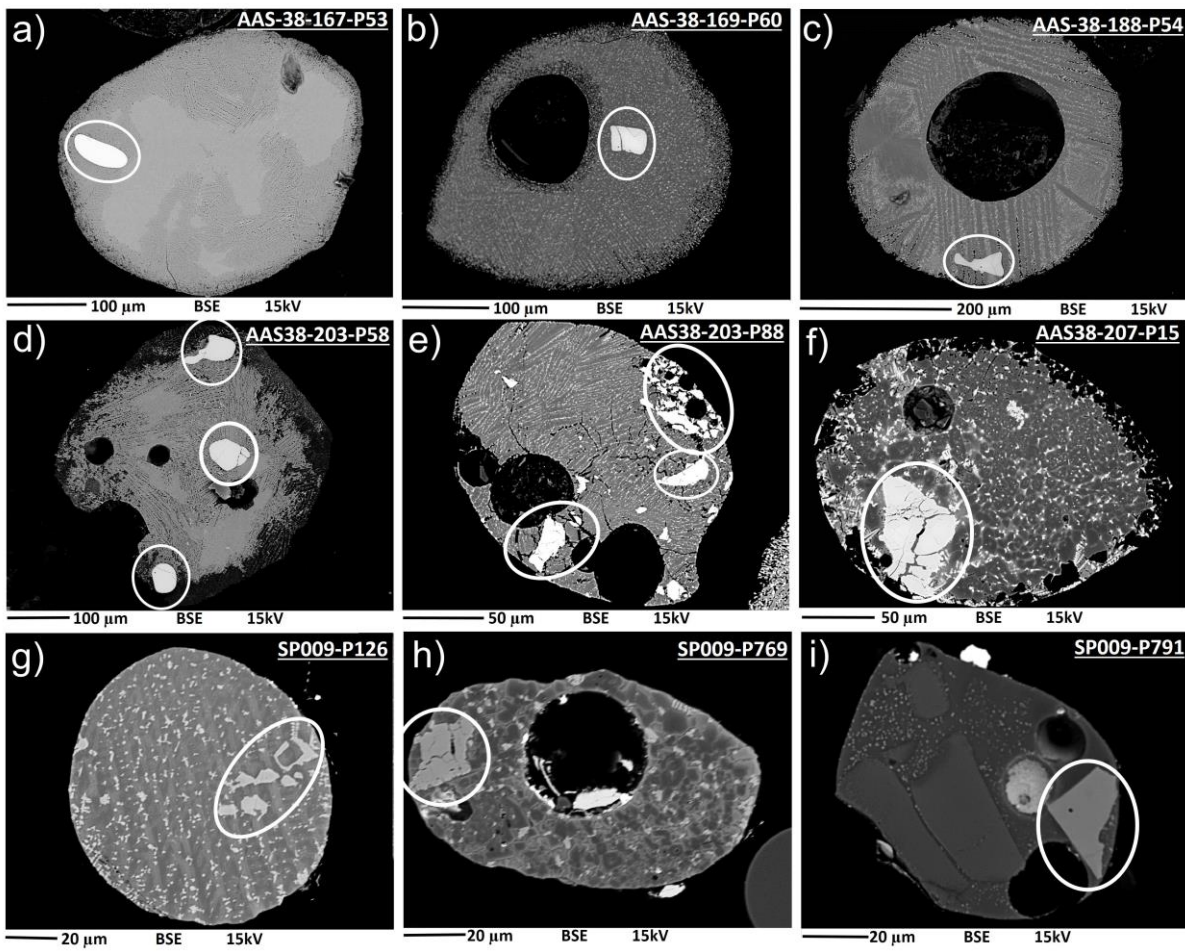


Fig. 2

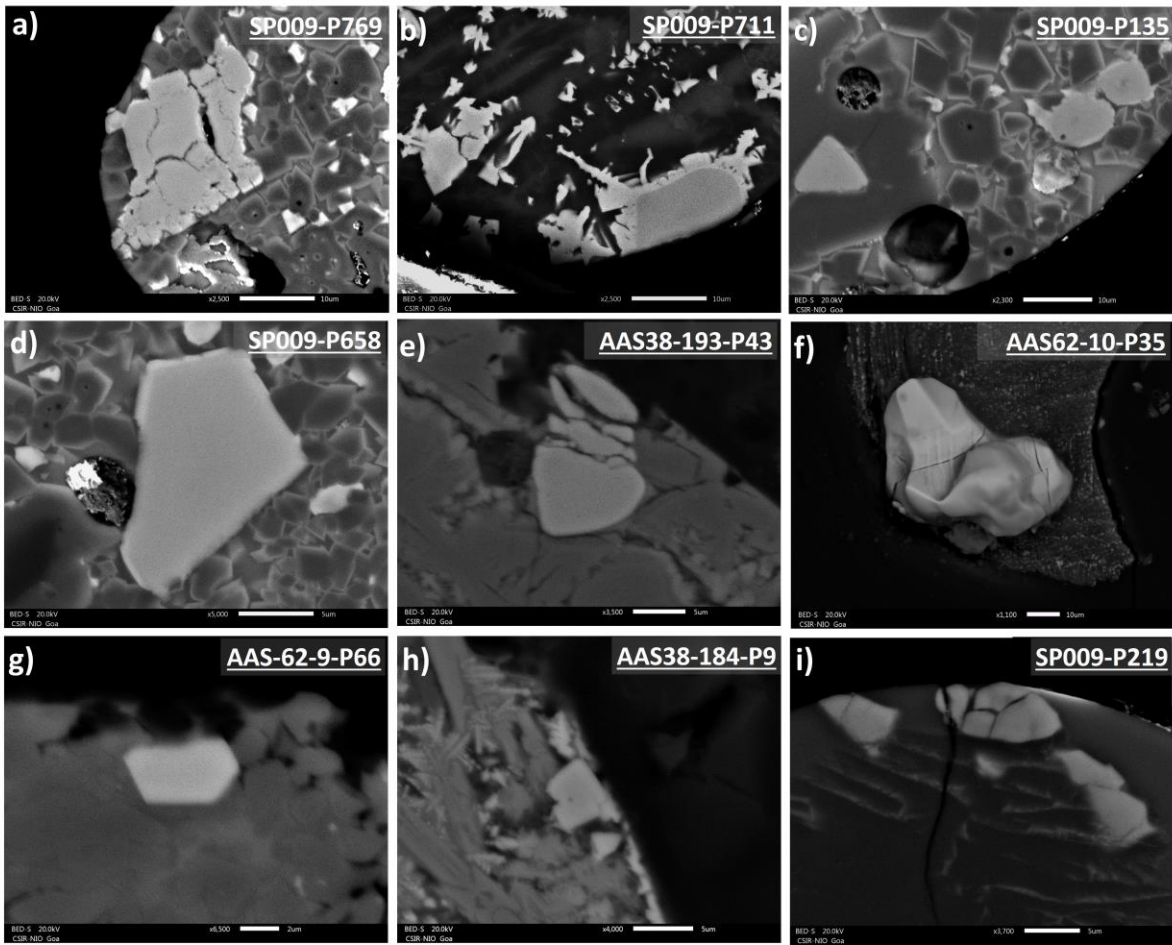


Fig. 3

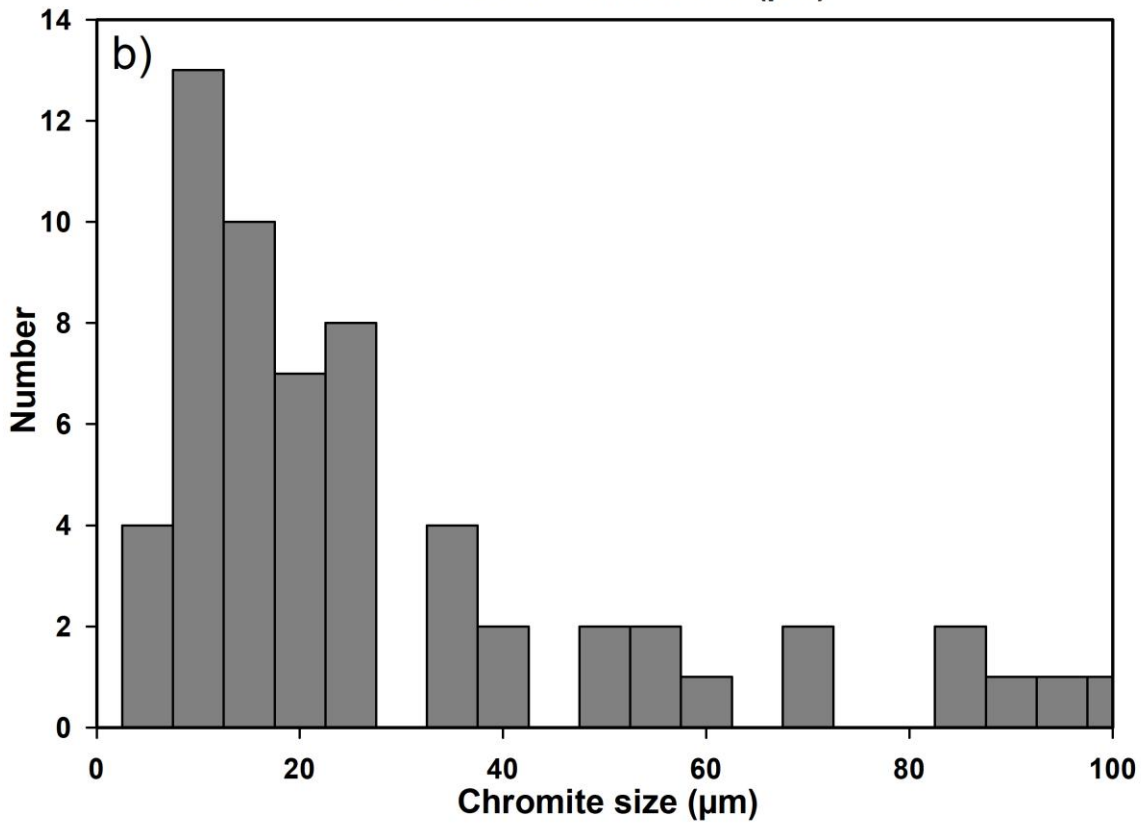
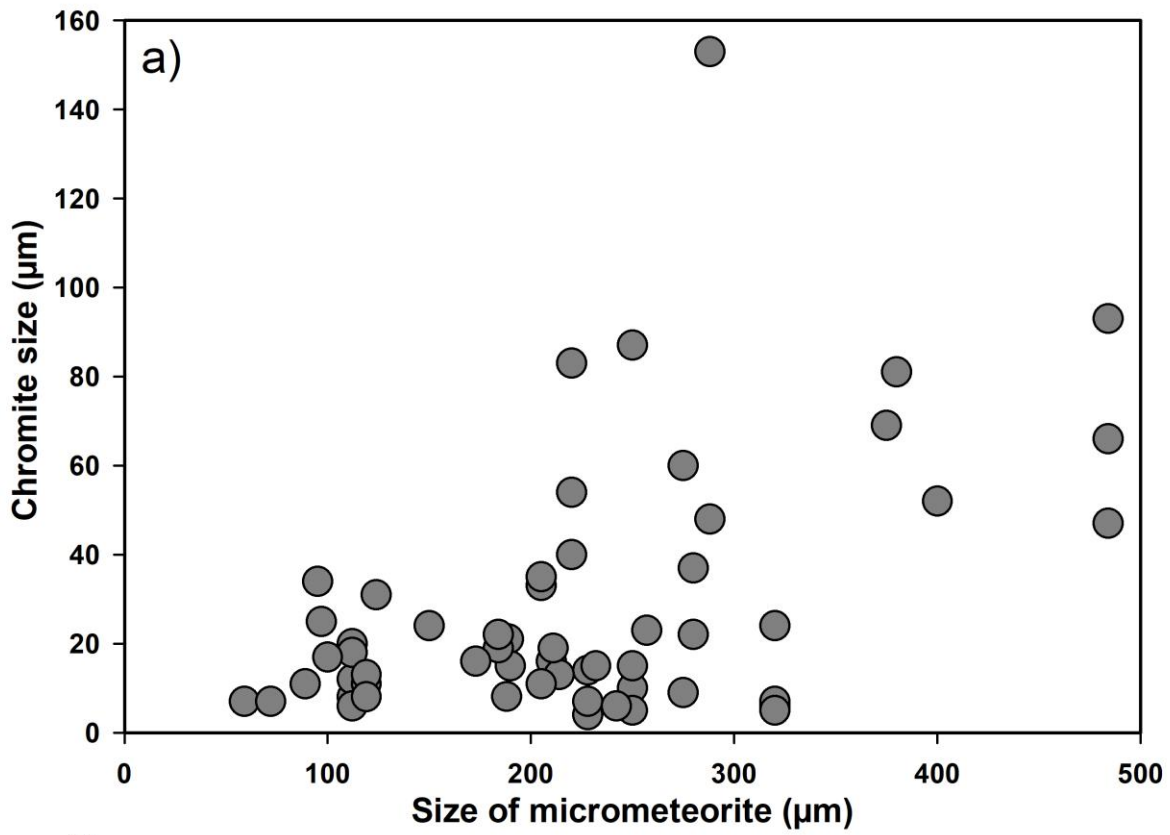


Fig. 4

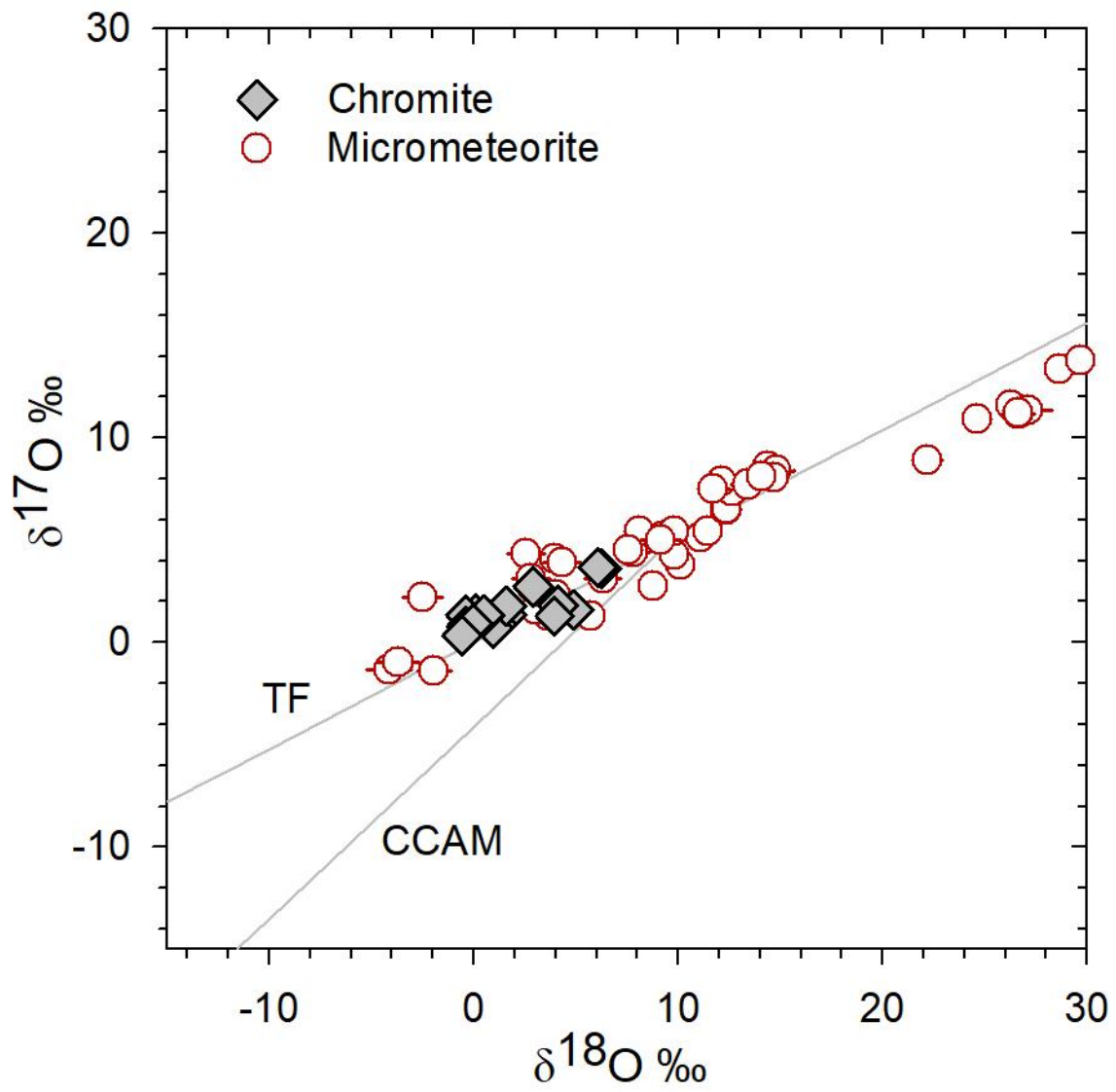


Fig. 5

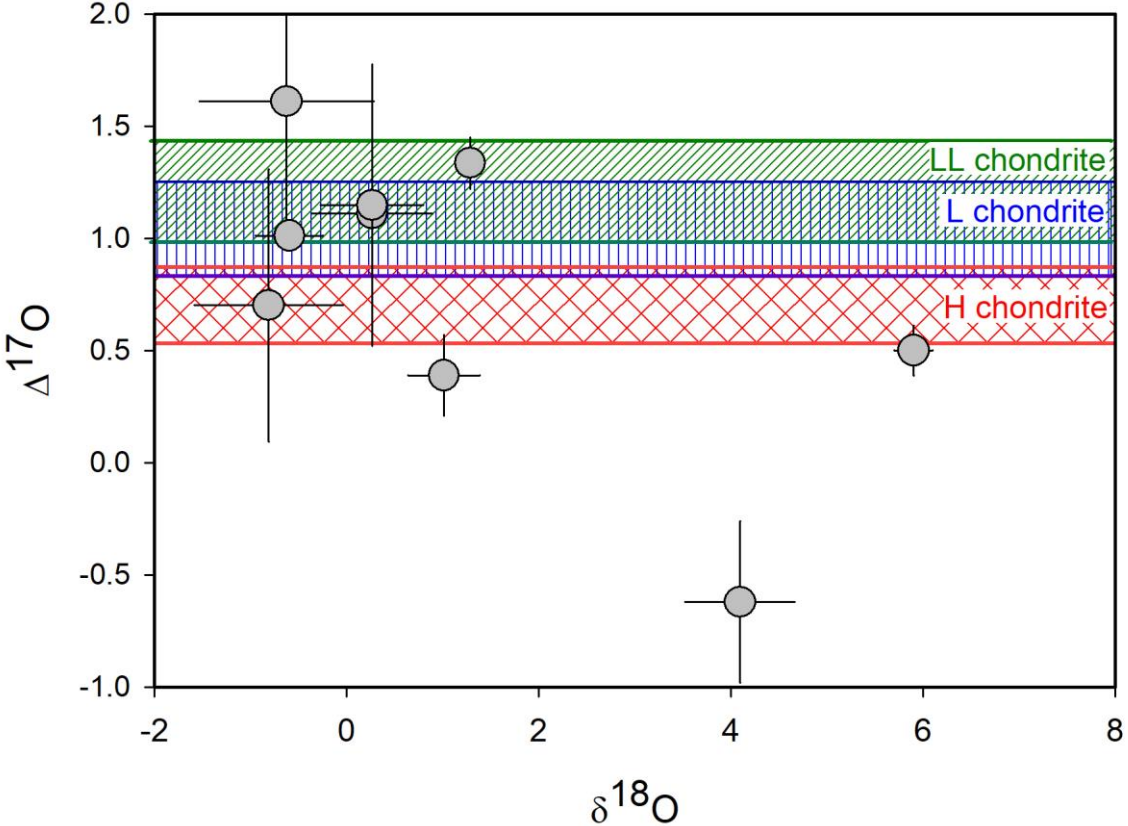


Fig. 6

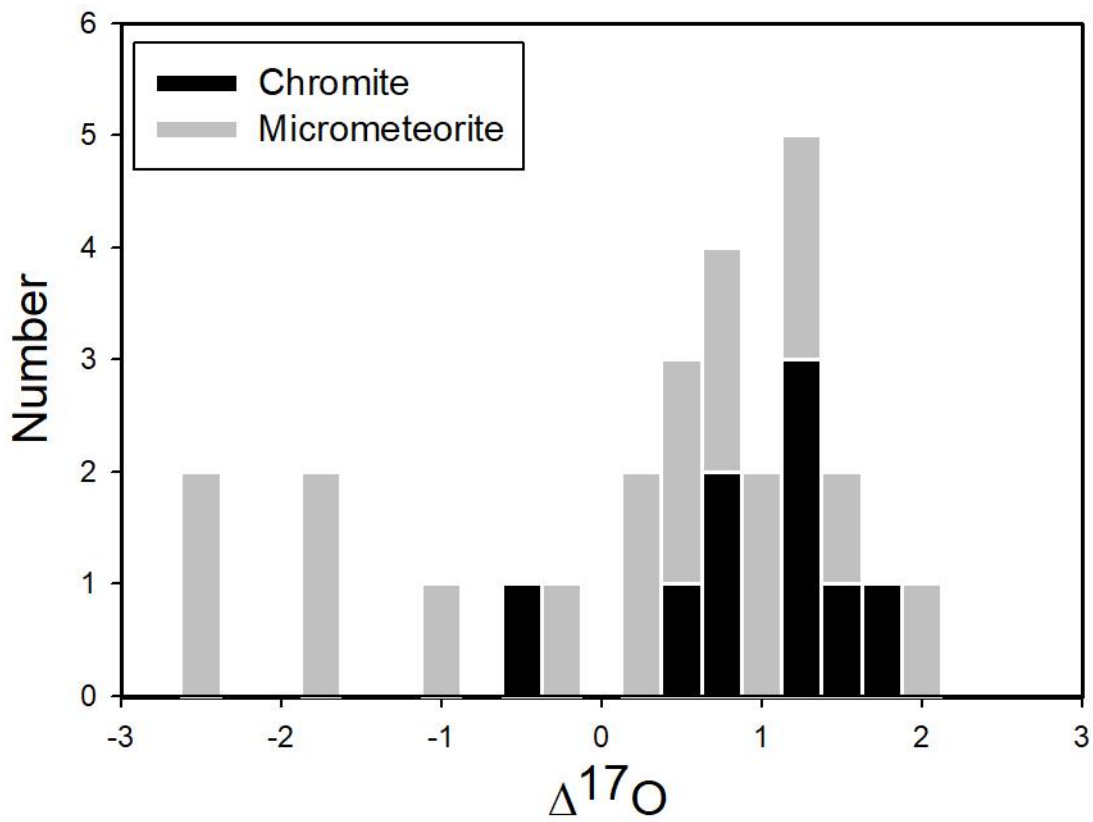


Fig. 7

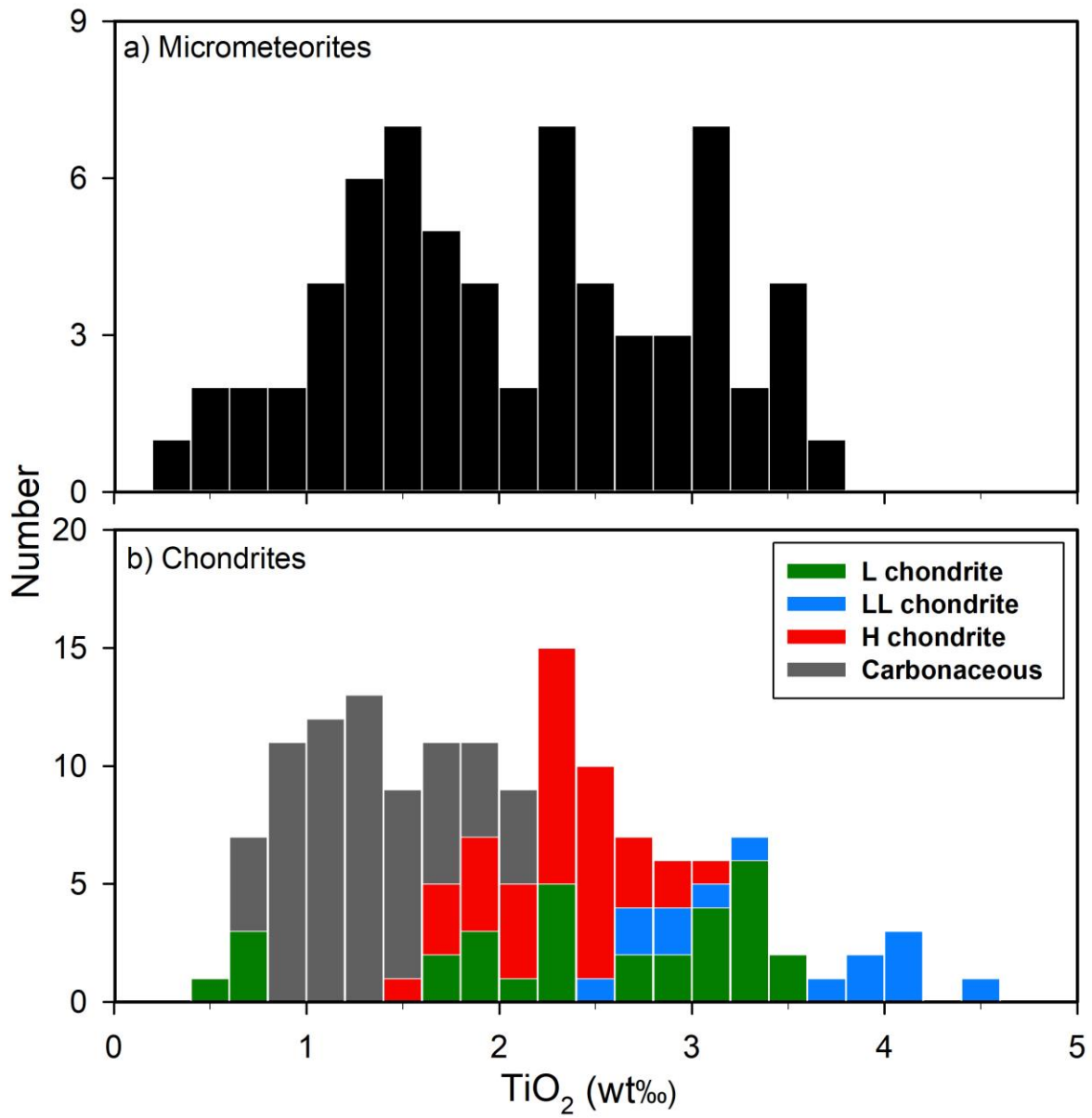


Fig. 8

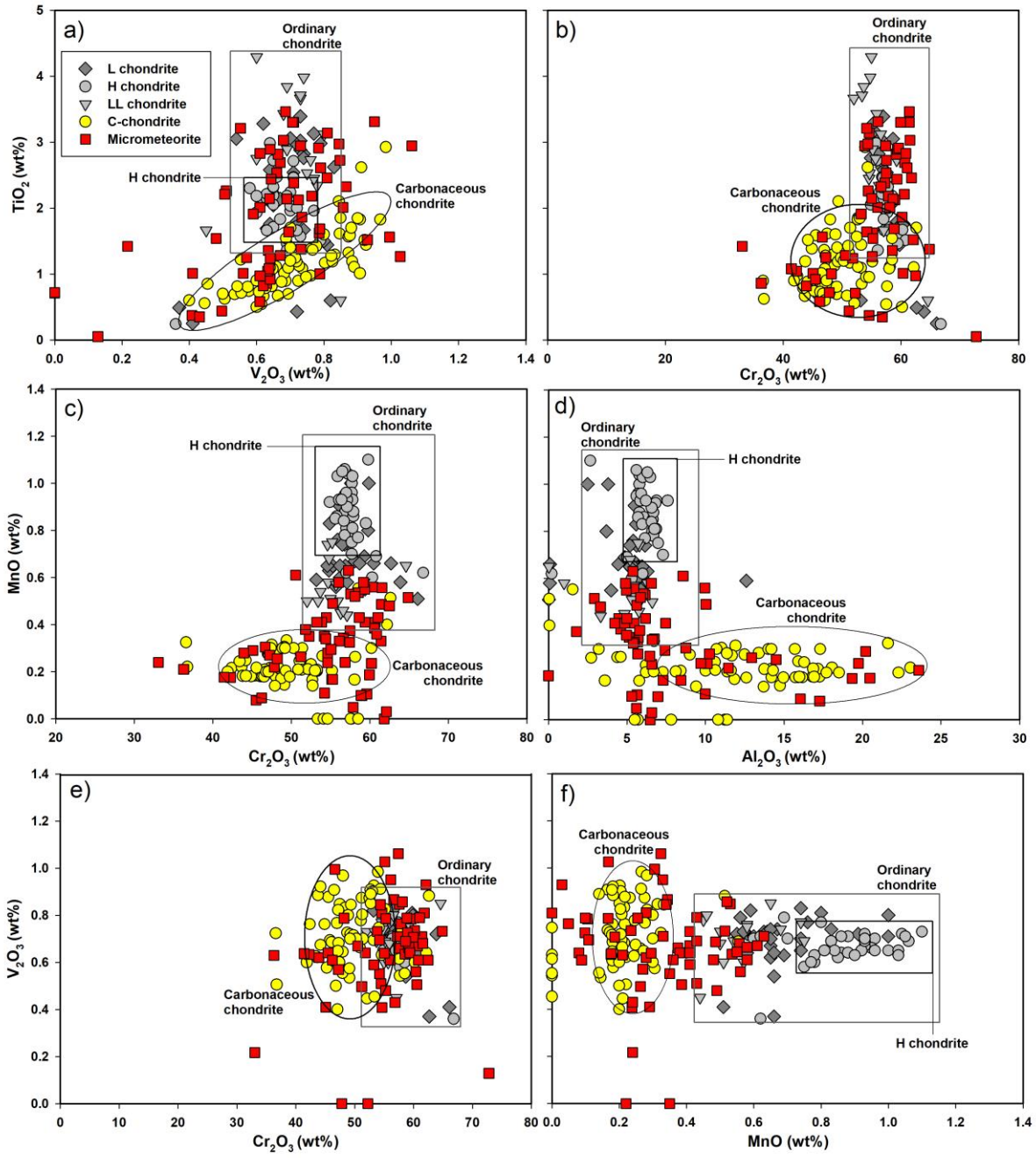


Table 1: Chemical composition (wt%) of the chromite grains from micrometeorites.

Sr. No	Cosmic spherule#	Type	Spherule size (μm)#	Chromite size(μm)*	MgO	Al ₂ O ₃	SiO ₂	CaO	TiO ₂	Cr ₂ O ₃	MnO	FeO	V ₂ O ₃	ZnO	Total
1	AAS-38-143-P141A	Barred	150	24	11.31	1.78	0.99	0.06	2.53	57.48	0.37	22.23	0.66	0.22	97.63
2	AAS-38-167-1-P20	Barred	280	37	6.50	5.62	0.10	0.00	3.46	61.45	0.49	22.79	0.69	0.00	101.09
				22	11.62	5.67	0.09	0.01	3.30	61.43	0.33	17.54	0.71	0.00	100.70
3	AAS-38-167-1-P59	Porphyritic	210	16	6.71	10.12	0.70	0.04	0.37	54.63	0.24	25.78	0.41	0.00	99.00
4	AAS-38-167-P53	Barred	380	81	2.51	6.16	0.05	0.00	2.73	57.55	0.53	28.51	0.85	0.24	99.14
5	AAS-38-169-P60	Barred	400	52	6.91	9.70	0.29	0.04	0.35	56.85	0.24	24.82	0.43	0.00	99.63
6	AAS-38-170-P89	Porphyritic	188	8.1	8.81	20.20	1.30	0.18	1.01	45.10	0.29	21.83	0.41	0.00	99.13
7	AAS-38-177-P51	Porphyritic	228	4	8.86	23.58	0.83	0.01	0.86	36.29	0.21	28.65	0.63	0.06	99.98
8	AAS-38-180-P73	Barred	320	24	3.29	6.55	0.03	0.01	2.01	56.04	0.58	28.55	0.61	0.23	97.90
9	AAS-38-180-P107	Barred	650	23	12.30	5.69	0.18	0.01	3.14	54.61	0.28	20.07	0.81	0.15	97.24
10	AAS-38-182-P25	Porphyritic	228	14	8.69	9.96	0.15	0.00	1.01	60.39	0.56	18.58	0.56	0.01	99.89
				7	10.68	4.47	1.26	0.07	2.26	54.47	0.43	23.07	0.51	0.00	97.22
11	AAS-38-184-P28	Barred	288	153	9.36	5.46	0.07	0.03	2.69	60.67	0.41	21.78	0.67	0.19	101.33
				48	12.36	4.61	0.59	0.02	2.21	60.58	0.39	19.99	0.51	0.10	101.32
12	AAS-38-184-P9	Barred	320	6	8.69	8.45	0.53	0.00	1.26	55.14	0.17	23.42	1.03	0.00	98.69
				7	9.35	6.02	0.79	0.08	1.36	58.56	0.54	21.78	0.63	0.00	99.10
				7	10.53	5.60	0.63	0.06	2.18	57.86	0.05	20.02	0.76	0.19	97.88
				5	11.86	7.31	0.67	0.10	1.62	55.28	0.17	20.12	0.79	0.33	98.23
13	AAS-38-188-P54	Barred	375	69	6.44	5.72	0.03	0.01	3.21	54.21	0.35	29.28	0.55	0.09	99.90
14	AAS-38-193-P40	Porphyritic	250	10	16.53	6.48	0.33	0.00	2.46	61.82	0.00	11.18	0.81	0.30	99.91
				15	16.70	6.57	0.69	0.02	1.86	60.20	0.24	10.67	0.73	0.24	97.92
				5	17.68	6.97	0.46	0.01	2.12	58.97	0.10	10.67	0.72	0.20	97.91

				5	16.83	6.58	0.65	0.09	1.52	62.10	0.03	10.80	0.93	0.36	99.90
15	AAS-38-193-P43	Porphyritic	214	13	10.13	0.00	0.00	0.03	3.30	59.95	0.19	23.75	0.71	0.12	98.18
16	AAS-38-193-P45		242	6	15.91	0.10	0.40	0.01	0.05	72.81	2.97	6.46	0.13	0.01	98.84
17	AAS-38-195-P80A	Barred	257	23	7.94	5.14	1.17	0.01	0.71	52.26	0.35	28.93	0.00	0.00	96.50
18	AAS-38-203-P58	Barred	484	93	5.86	5.43	0.07	0.01	3.03	61.56	0.56	23.44	0.68	0.17	100.81
				66	4.99	4.97	0.86	0.04	2.44	59.34	0.55	25.44	0.64	0.18	99.46
				47	7.23	4.91	0.16	0.00	2.82	59.20	0.58	23.39	0.66	0.13	99.07
19	AAS-38-203-P88	Barred	205	33	10.14	4.86	0.55	0.02	2.89	59.40	0.41	21.41	0.64	0.09	100.41
				35	5.42	5.37	0.94	0.03	2.38	57.29	0.63	25.37	0.71	0.27	98.41
				11	7.15	4.99	1.08	0.04	2.14	58.65	0.43	24.77	0.69	0.19	100.13
20	AAS-38-204-P58	Cryptocrystalline	189	21	13.22	5.65	0.36	0.01	2.91	59.61	0.11	17.74	0.78	0.11	100.49
21	AAS-38-207-P15	Porphyritic	250	87	4.83	6.18	0.13	0.03	2.61	61.04	0.43	24.77	0.79	0.21	101.02
22	AAS-38-207-P117	Porphyritic	250	100	7.63	6.74	0.19	0.01	2.32	56.65	0.34	24.99	0.87	0.24	99.99
23	AAS-62-5-P77	Barred	190	15	6.54	5.47	0.23	0.04	3.31	56.11	0.33	23.67	0.95	0.29	96.95
24	AAS-62-10-P35	Barred	275	60	8.53	5.86	0.35	0.03	2.01	58.11	0.52	21.17	0.86	0.18	97.62
25	AAS-62-26-P86	Porphyritic	184	19	16.42	5.31	0.90	0.01	1.68	58.86	0.10	14.73	0.79	0.30	99.10
				22	8.09	2.92	0.44	0.16	1.38	64.87	0.51	19.71	0.73	0.13	98.93
26	AAS-62-26-P132	Porphyritic	220	83	7.21	5.40	0.15	0.01	2.94	57.42	0.32	23.40	1.06	0.32	98.24
				54	8.62	7.47	0.15	0.04	2.94	53.85	0.41	24.77	0.73	0.16	99.13
				40	8.50	6.61	0.21	0.00	2.97	54.40	0.34	22.98	0.84	0.20	97.06
27	AAS-62-32-P102	Porphyritic	173	16	2.76	8.75	0.79	0.02	1.56	46.66	0.31	37.66	1.00	0.00	99.49
28	AAS-62-32-P106	Scoriaceous	232	15	5.45	11.46	0.60	0.05	0.72	47.83	0.22	32.69	0.00	0.00	99.02
29	AAS-62-51-P4	Porphyritic	211	19	11.22	19.74	0.27	0.03	1.42	33.06	0.24	30.64	0.22	0.00	96.84
30	AAS-62-51-P52	Porphyritic	275	9	6.74	10.25	1.46	0.01	0.82	43.94	0.28	31.97	0.62	0.00	96.09
31	SP009-P126	Cryptocrystalline	112	8	7.49	7.41	0.22	0.11	2.14	55.04	0.29	24.83	0.64	0.02	98.20
				12	7.13	4.22	0.93	0.06	1.91	53.25	0.41	26.85	0.59	0.04	95.39
				20	8.47	5.81	1.98	0.09	1.24	51.81	0.38	24.69	0.64	0.00	95.11

				6	9.30	6.45	1.37	0.12	1.25	47.25	0.27	27.83	0.57	0.01	94.42
				18	9.00	9.98	0.51	0.11	1.64	54.21	0.11	23.06	0.70	0.00	99.31
32	SP005-P135	Porphyritic	119	11	8.58	17.27	0.58	0.00	0.92	45.49	0.08	25.21	0.64	0.05	98.82
				13	7.95	19.34	0.56	0.00	1.04	42.28	0.18	25.40	0.63	0.00	97.38
				8	7.82	20.47	0.41	0.00	1.08	41.41	0.18	25.97	0.64	0.00	97.97
33	SP005-P219	Glass	89	12	8.39	8.57	1.46	0.54	1.28	50.55	0.61	27.87	0.67	0.05	99.99
				10	6.75	9.45	1.10	1.00	1.62	47.36	0.66	27.73	0.45	0.00	96.13
				7	6.51	9.02	1.41	0.36	1.02	50.25	0.57	29.06	0.47	0.02	98.69
34	SP005-P325	Porphyritic	59	7	10.03	10.03	0.75	0.07	1.54	55.26	0.49	18.77	0.48	0.00	97.42
35	SP005-P530	Glass	72	7	13.05	4.97	0.10	0.03	2.83	60.86	0.36	13.56	0.61	0.00	96.37
36	SP005-P658	Porphyritic	100	17	4.29	14.51	0.34	0.04	1.00	48.20	0.26	28.87	0.79	0.00	98.29
37	SP005-P711	Porphyritic	97	25	7.86	12.93	0.22	0.13	0.44	51.21	0.26	24.42	0.50	0.00	97.97
38	SP005-P769	Porphyritic	124	31	6.39	16.05	0.59	0.00	0.58	46.21	0.09	27.31	0.61	0.07	97.91
39	SP005-P791	Porphyritic	95	34	4.61	3.31	0.21	0.02	0.97	62.48	0.48	26.38	0.61	0.00	99.07
40	SP007-P72	Relict bearing	132	7	6.80	12.14	0.84	0.13	1.59	46.40	0.12	30.45	0.90	0.01	99.36
41	SP007-P2	Unmelted	153	14	2.81	6.01	0.28	0.05	2.03	53.25	0.10	33.88	1.00	0.30	99.71
42	SP007-P29	Relict bearing	74	6	9.55	13.69	0.29	0.05	1.21	49.56	0.31	24.34	0.28	0.01	99.27

indicate spherule size as diameter

* indicate chromite size measured along the maximum length.

All measurements are in wt%

Table 2. Oxygen isotopic composition of chromites and the olivine phases in micrometeorites. All the values of the oxygen isotopic composition are reported in ‰. Serial No. 11 to 18 are micrometeorites where chromite could not be analyzed.

#	Name	Type	Spot#	$\delta^{18}\text{O}$	2 σ	$\delta^{17}\text{O}$	2 σ	$\delta^{17}\text{O}$	2 σ
1	SP005-P126	Glass	1	5.8	0.6	1.3	0.5	-1.7	0.6
			2	8.8	0.7	2.7	0.5	-1.8	0.6
			3	10.2	0.6	3.8	0.5	-1.5	0.6
			4	9.9	0.7	4.3	0.4	-0.9	0.5
			5	11.2	0.8	5.2	0.4	-0.7	0.5
			6	11.5	0.5	5.4	0.5	-0.5	0.5
2	SP005-P219	Glass	*1	4.7	0.9	1.5	0.4	-0.9	0.6
			*2	3.9	0.7	1.7	0.4	-0.3	0.6
			*3	3.7	0.6	1.2	0.4	-0.7	0.5
			4	3.7	0.8	1.3	0.5	-0.6	0.6
			5	6.4	0.9	3.1	0.3	-0.2	0.6
3	AAS-38-203-P58	Barred	*1	1.4	0.7	1.3	0.4	0.6	0.5
			*2	0.9	0.5	0.8	0.5	0.3	0.5
			*3	0.7	0.7	0.6	0.4	0.3	0.6
			4	12.4	0.7	6.5	0.5	0.0	0.6
			5	12.4	0.7	6.5	0.5	0.1	0.6
4	AAS-38-203-P88	Barred	*1	6.0	0.7	3.6	0.5	0.4	0.6
			*2	1.4	0.6	1.7	0.4	1.0	0.5
			*3	5.8	0.6	3.6	0.4	0.6	0.5
			4	7.9	0.8	4.4	0.4	0.3	0.6
			5	8.2	0.7	5.5	0.5	1.2	0.6
			6	9.4	0.7	5.2	0.5	0.4	0.6
5	AAS-38-207-P15	Barred	*1	2.7	0.4	2.7	0.6	1.3	0.6

			*2	-0.1	0.4	1.3	0.6	1.4	0.6
			3	7.6	0.7	4.5	0.5	0.6	0.6
			4	9.9	0.6	5.4	0.5	0.3	0.6
6	AAS-38-169-P60	Barred	*1	-0.6	0.9	1.3	0.4	1.6	0.6
			2	12.7	0.8	7.4	0.5	0.8	0.7
			3	12.2	0.6	7.9	0.5	1.5	0.6
7	AAS-38-188-P54	Barred	*1	0.3	0.6	1.2	0.5	1.1	0.6
			2	13.5	0.8	7.7	0.5	0.7	0.6
			3	11.8	0.8	7.5	0.5	1.4	0.6
8	AAS-38-167-1-P20	Barred	*1	0.3	0.5	1.3	0.6	1.1	0.6
			2	14.5	0.8	8.6	0.5	1.1	0.6
			3	14.9	0.8	8.4	0.5	0.7	0.7
9	AAS-38-167-P53	Barred	*1	-0.6	0.6	0.7	0.4	1.0	0.5
			*2	-0.2	0.6	0.9	0.5	1.0	0.6
			3	14.7	0.7	8.1	0.5	0.4	0.6
			4	14.2	0.6	8.1	0.5	0.8	0.6
10	AAS-38-204-P58	Barred	*1	-0.8	0.8	0.3	0.5	0.7	0.6
			2	-1.9	0.8	-1.4	0.5	-0.4	0.7
			3	-4.1	1.1	-1.3	0.6	0.8	0.8
11	SP005-P135	Porphyritic	1	26.5	0.8	11.5	0.4	-2.3	0.6
			2	26.4	0.7	11.6	0.4	-2.1	0.5
			3	30.7	0.6	13.6	0.4	-2.3	0.5
			4	28.7	0.7	13.4	0.4	-1.6	0.6
			5	29.8	0.6	13.8	0.4	-1.7	0.5
12	SP005-P658	Porphyritic	1	22.3	0.7	8.9	0.5	-2.7	0.6
			2	27.2	1.2	11.4	0.7	-2.7	0.9
13	SP005-P711	Glass	1	26.7	0.8	11.2	0.4	-2.7	0.6
			2	26.7	0.7	11.2	0.4	-2.6	0.5

14	SP005-P769	Porphyritic	1	24.7	0.7	10.9	0.5	-1.9	0.6
15	SP005-P770	Unmelted	1	3.0	0.6	2.8	0.3	1.2	0.4
			2	2.9	0.5	2.8	0.4	1.3	0.5
16	SP007-P72	Relict bearing	1	-3.6	1.0	-1.0	0.5	0.9	0.7
			2	3.1	0.9	1.6	0.5	0.0	0.7
			3	9.2	1.0	5.0	0.6	0.2	0.8
17	SP007-P2	Unmelted	1	4.0	0.7	4.1	0.5	2.0	0.6
			2	4.4	0.9	3.9	0.5	1.6	0.7
			3	-2.4	1.0	2.2	0.6	3.5	0.8
			4	2.6	0.9	4.3	0.3	3.0	0.6
18	SP007-P29	Relict bearing	1	3.3	0.6	2.5	0.5	0.8	0.6
			2	4.1	0.7	2.4	0.5	0.2	0.6
			3	2.9	0.9	3.1	0.6	1.6	0.7

* marked are the oxygen isotope analyzed for chromite grain.